10TH INTERNATIONAL SYMPOSIUM ON PARTICLE IMAGE VELOCIMETRY – PIV13
Delft, The Netherlands, July 2-4, 2013

Evaporation-induced flows in confined droplets of diluted aqueous NaCl solution

Yong-Seok Choi[1], Kyeong-Won Seo[2], Sang-Joon Lee[3], Seong-Hun Kim[4] and Ju-Hyeon Yun[5]

[1,4,5] Fluid System Design Division, Korea Atomic Energy Research Institute, Daejeon, Korea
cys@kaeri.re.kr

[2,3] Department of Mechanical Engineering, Pohang University of Science and Technology, Pohang, Korea

ABSTRACT

The flows in a naturally evaporating liquid droplet confined by two flat plates were investigated experimentally. A diluted sodium-chloride (NaCl) aqueous solution was used to form the confined droplets. The evaporation of water at the free surface of the droplet built up a concentration gradient inside the solution, which induced a natural convection flow. Three-dimensional trajectories of tracer particles in the droplet were tracked, and the corresponding velocity fields were obtained by using a digital in-line holographic microscopy technique. Furthermore, this study investigated the effects of the confined droplet's aspect ratio and the liquid's molar concentration on the evaporation-induced flows in the droplet.

1. Introduction

Fluid motion inside a naturally evaporating sessile droplet is one of the most interesting topics in the field of physicochemical research. Deegan et al. [1, 2] studied outward capillary flows inside evaporating droplets with pinned contact lines. Their research observations included the induction of flows to compensate for the liquid loss at the edge of evaporating droplets. The study also explained why the contaminants in the evaporating droplets form ring-like depositions. Hu and Larson [3] numerically analyzed the time-dependent axisymmetric outward flow in an evaporating sessile droplet with a pinned contact line. Savino and Monti [4] numerically investigated the natural and Marangoni-induced convection flows inside sessile and pendant droplets of half- and full-sphere configurations. Their report shows that natural convection dominates the solute transport inside the droplets. Kang et al. [5, 6] also experimentally and numerically observed the convection inside evaporating droplets of a water-alcohol mixture and a water-salt solution placed on a hydrophobic substrate. Their work demonstrates that the evaporation of a droplet is accompanied by a convective motion that is an important factor in the overall mass transport phenomenon.

Clément and Leng [7] first investigated the evaporation of liquids in confined droplets. They measured the diffusion coefficient of the evaporating gas by observing the temporal variations in the solvent volume. In addition, Daubersies and Salmon [8] numerically studied the drying process of solutions as well as the colloidal dispersion from droplets in a confined geometry. However, these studies were conducted by using one-dimensional simple transport equations with the assumption that that the liquid layer is very thin.

In this study, droplets with considerable thickness in a confined geometry are investigated. We measured the convection flows formed in the slowly evaporating confined droplets of diluted aqueous sodium-chloride (NaCl) solutions. The 3D trajectories of tracer particles inside the droplet are measured by using digital holographic particle tracking velocimetry (DH-PTV), after which the flow fields are deduced. To the best of the authors' knowledge, this study is the first effort to measure the evaporation-induced convection flow inside a confined droplet.

2. Experimental Methods

2.1. Materials and conditions

A NaCl solution diluted with deionized (D.I.) water was used to form a liquid droplet. The molar concentration of the diluted solution was varied to 0.1, 0.5, and 1 M. Polystyrene micro particles with a mean diameter of 4 μm were seeded in the solution as flow tracers. Using a micropipette, a small amount of the solution was placed between two slide glasses that are separated by a spacer to form a confined droplet. The initial volume of the confined droplets tested in this study ranged from 1 μL to 20 μL.

The slide glasses were spin-coated with polydimethylsiloxane (PDMS) to make the surface hydrophobic and to increase the contact angle. This surface treatment enabled the confined droplet to have an approximately 90° contact angle at the edges, which resulted in an almost rectangular cylindrical shape. The heights (H) of the confined droplet

varied between 0.5 and 2.0 mm. The viscosity of the tested fluid was approximately ν = 0.94 mm^2/s. The room temperature was maintained at 25 ℃ ± 1 ℃.

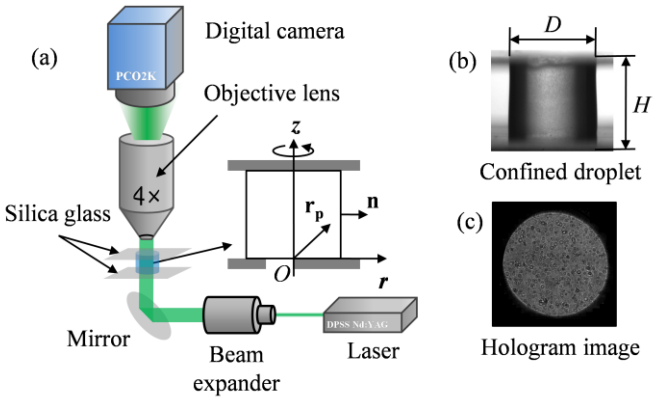

Figure 1. (a) Schematic of the experimental setup. (b) Side view of the confined droplet. (c) A typical hologram image captured in this study.

2.2. Measurement of droplet volume

The volume of the evaporating droplet was evaluated quantitatively from the optical images obtained from the lateral direction. The droplet images were consecutively recorded, and the transient volume variation of the droplet was estimated with the assumption that the droplet has an axisymmetric geometry. As the evaporation proceeded, the diameter of the confined droplet slowly shrunk while the contact angle was maintained. The receding velocity of the evaporating surface was measured by tracing the wall position from the images.

2.3. 3D flow field measurement

The in-line DHPTV setup is employed to obtain 3D, three-component velocity vector field information. The setup comprised a continuous diode-pumped solid-state Nd:YAG laser (λ = 532 nm, 100 mW, CrystaLaser, USA), a beam expander (20×, Newport, USA), a microscope objective lens (4×, NA=0.1, Nikon, Japan), and a digital camera (PCO.2000, PCO, Germany). The focal plane of the objective lens was positioned above the top substrate to generate holographic images and to obtain the overlap of the scattered and unscattered waves. The holographic images magnified by the objective lens were captured by using the digital camera and then stored in a computer hard disk. The 3D motion of the flow tracers inside the confined droplet was analyzed by employing the digital image processing techniques described in our previous work [9, 10].

The flow motion was immediately initiated after the confined-droplet was formed, and a stable flow pattern was established after approximately 1 min. The holograms were recorded consecutively for 10 min after the stable flow patterns settled.

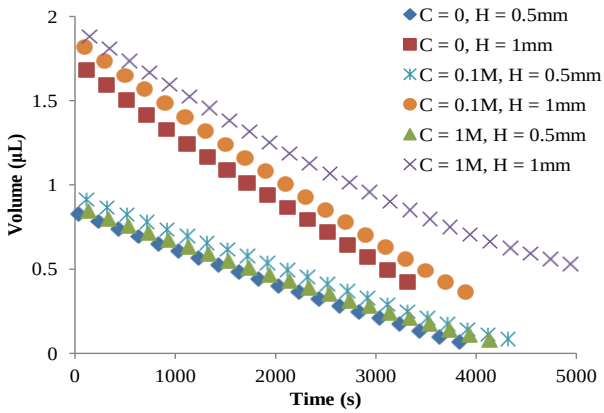

Figure 2. Temporal volume of the evaporating confined droplets.

3. Results

Figure 2 shows the temporal volume variations of the confined droplets of C = 0, 0.1, and 1 M and H = 0.5 and 1 mm. The inclination of the volume profiles indicates the evaporation rate. Except for C = 1 M, the evaporation rates are nearly constant. In addition, the rates are proportional to the droplet height H. The evaporation rate for H = 1 mm cases are nearly twice that of H = 0.5 mm cases. The evaporation rate is proportional to the gap distance because the evaporation of the confined droplet is governed by the vapor diffusion along the gap between the two substrates. When C = 1 M, the decrease in the evaporation rate is evident as the confined droplet evaporates. This decrease in evaporation rate is caused by the increase in vapor pressure at the liquid surface that can be attributed to the increased number of ion molecules that pulls the polarized water molecules.

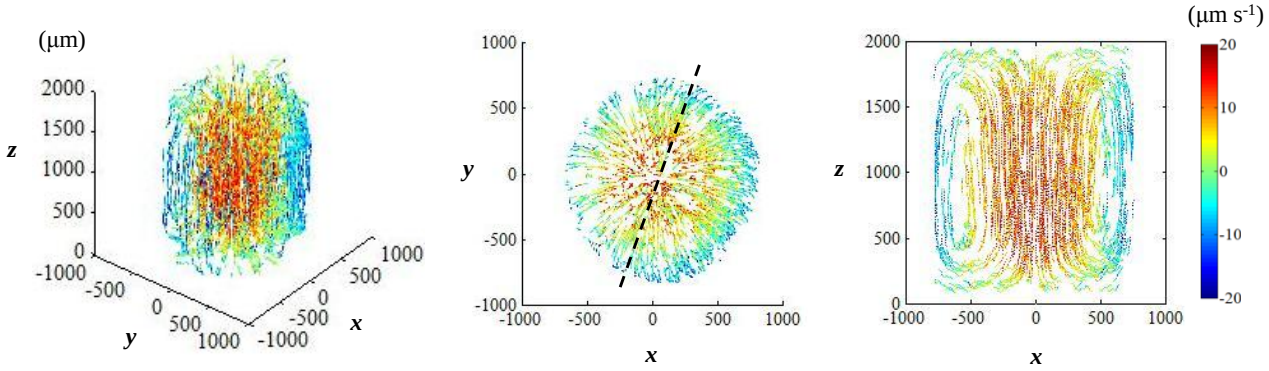

Figure 3. Trajectories of tracer particles in the confined droplet: H = 2 mm, V = 5 μL, and C = 1 M.

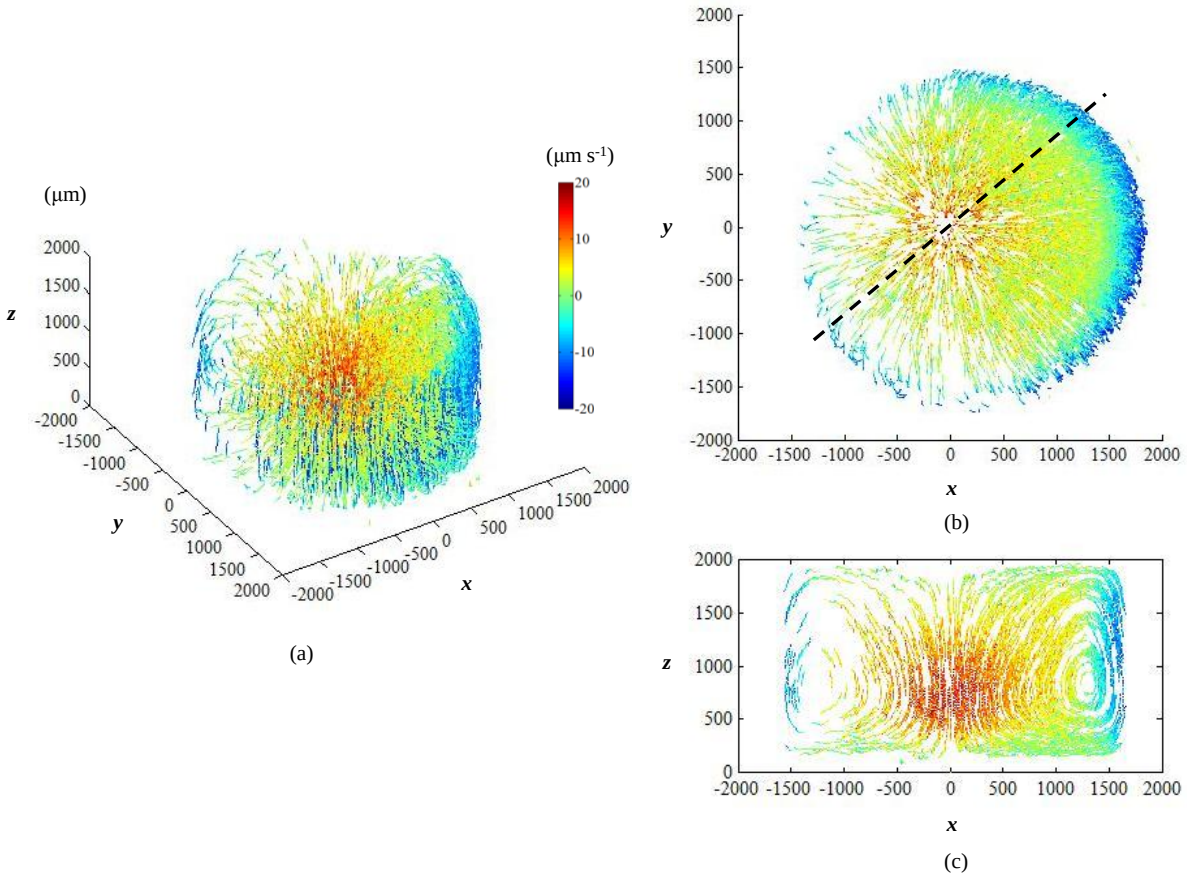

Figure 4. Trajectories of tracer particles in the confined droplet: H = 2 mm, V = 20 μL, and C = 1 M.

Figure 3 shows the trajectories of the tracer particles suspended in the confined droplet with a height of H = 2 mm, an initial volume of V = 5 μL, and a molar concentration of C = 1 M. The axial velocities are coded in color, with red and blue indicating upward and downward motions, respectively. The axial velocities are upward in the central region and downward in the outer region. To satisfy the condition of continuity, the flow is directed outwards near the top and inwards near the bottom. In general, the axisymmetric convection motion is the dominant flow. On the contrary, no noticeable convective motion is observed when we tested the confined droplet of D.I. water. Therefore, the temperature gradient induced by the latent heat of evaporation is negligible because the surface evaporation rate of the diluted aqueous NaCl solution is almost the same as that of purified water. The Marangoni effect attributed to the temperature and concentration gradients was not considered to simplify the study. The outward capillary flows observed in the previous studies [1-3] were not observed because the contact lines were not pinned given the hydrophobic surface condition.

The trajectories of the tracer particles in the confined droplet of H = 2 mm, V = 20 μL, and C = 1 M are shown in Fig. 4. The convectional flow motion is similar to that of the previous case, except for the asymmetry along the z-axis shown in the x-z plane view. The region of fast upward motion is adjacent to the bottom surface compared with the previous case. Accordingly, the trajectories are more tightly packed in the region near the center of the bottom surface than those near the top surface. A slight asymmetry is also observed in the x-y plane. However, this asymmetry seemed to originate from uncontrollable conditions such as the slightly different evaporation rates around the surface and the misalignment of two substrates.

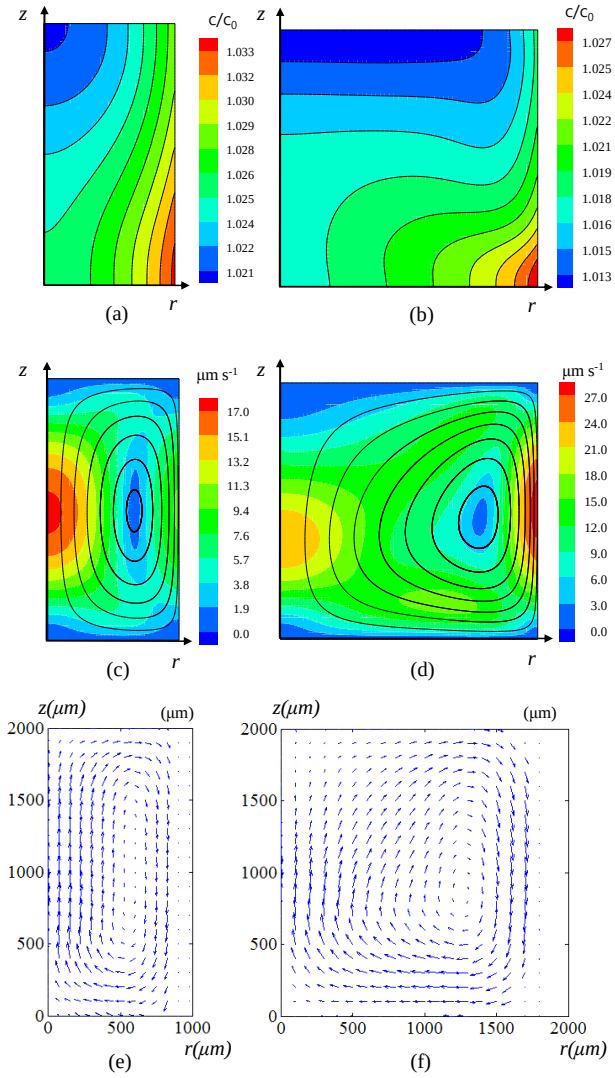

Figure 5. (a–d) Spatial distributions of concentration and flow speed obtained from the numerical simulation: (e–f) velocity vector fields obtained from the experiment; (a, c, e) *H* = 2 mm, *V* = 5 μL, and *C* = 1 M; (b, d, f) *H* = 2 mm, *V* = 20 μL, and *C* = 1 M.

4. Numerical Analysis

We conducted a numerical analysis on the flow field and concentration distribution inside the slowly evaporating confined droplet to confirm the underlying base physics. The stretching coordinate method introduced by Kang et al. [5] was employed to account for the effect of boundary shrinkage attributed to evaporation. The geometric boundary and concentration distribution of the evaporating confined droplet were assumed to be cylindrical and axisymmetric, respectively. The thermal convection and Marangoni effects were disregarded.

The local density variation attributed to the concentration gradient was estimated by employing the Boussinesq approximation in the Navier–Stokes equations [4, 5]. FLUENT (VERSION 6.3) with 2D axisymmetric unsteady model was employed for the numerical calculations.

5. Discussions

The spatial distributions of the concentration and flow field obtained from the numerical simulation and from the experiment for the H = 2 mm and C = 1 M cases are compared in Fig. 5. The experimental velocity field is obtained by the ensemble averaging of the particle velocities at each grid position (r, z). The streamlines of the numerical results show good agreement with the flow patterns obtained from the experiment. In the case of V = 5 μL, the flow patterns in the upper and lower parts are nearly symmetric. However, for V = 20 μL, the upward flow near the center axis decelerates after passing the midline. The different flow patterns are primarily attributed to the wide region of radially quasi-equivalent concentrations above the midline. In Figs. 5(b) and (d), the concentration and axial velocity profiles show different patterns according to the confined droplet configuration. As mentioned in V = 20 μL, a plateau is observed in the concentration profiles and the axial velocities are suppressed in the region of r/R < 0.8. In addition, the stagnation point where the axial velocity is $u_z = 0$ moves toward the evaporation surface as the diameter of the confined droplet increases, resulting in smaller axial velocities at r/R < 0.8. These results show the importance of the reciprocal interaction between the concentration distribution and the self-induced convection flow in this kind of physical model.

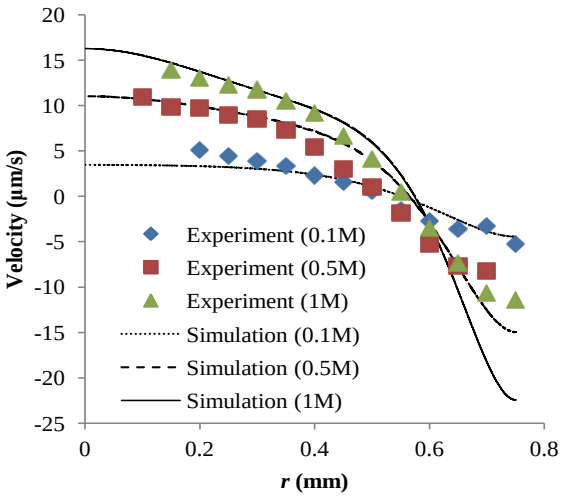

Figure 6. Axial velocity profiles along the midline z/Z = 0.5 at different ion concentrations. The convection velocity increases, as the molar concentration increases. The experimental data and simulation results exhibit larger deviations at higher concentrations especially near the free surface of the confined droplet. *H* = 0.5 mm and *V* = 1 μL.

Figure 6 compares the axial velocity profiles extracted from the midline z/Z = 0.5 of the confined droplets at different ion concentrations. Droplets that have the same geometry of V = 1 μL and H = 0.5 mm were tested with variations in molar concentrations of C = 0.1, 0.5, and 1 M. As the molar concentration increases, convection velocity also increases. The simulated velocity profiles are in good agreement with the experimented values when the concentration is low. As the ion concentration increases, however, both profiles show large deviations, especially near the outer edge of the confined droplet. These large deviations seem to be resulted from the neglected effect of surface tension gradient.

Acknowledgment

This work was supported by the National Research Foundation (NRF) of Korea grant funded by the Korea government (MEST) (No. NRF-2012M2C1A1026909). This work was supported by the Creative Research Initiatives (Diagnosis of Biofluid Flow Phenomena and Biomimic Research) of the NRF of Korea grant funded by the MEST.

REFERENCES

[1] Deegan RD, Bakajin O, Dupont TF, Hurber G, Nagel SR, Witten TA "Capillary flow as the cause of ring strains from dried liquid drops" Nature 389 (1997) 827-829

[2] Deegan RD, Bakajin O, Dupont TF, Hurber G, Nagel SR, Witten TA "Contact line deposits in an evaporating drop" Physical Review E 62 (2000) 756-765

[3] Hu H, Larson RG "Analysis of the microfluid flow in an evaporating sessile droplet" Langmuir 21 (2005) 3963-3971

[4] Savino R, Monti R "Buoyancy and surface-tension-driven convection in hanging-drop protein crystallizer" Journal of Crystal Growth 165 (1996) 308-318

[5] Kang KH, Lee SJ, Kang IS, Lee CM "Natural convection inside slowly evaporating droplets of aqueous solution of salt" In: Proceedings of 6th KSME-JSME Thermal and Fluids Engineering Conference, Jeju, Korea (2005)

[6] Kang KH, Lee SJ, Lee CM, Kang IS "Quantitative visualization of flow inside an evaporating droplet using the ray tracing method" Measurement Science and Technology 15 (2004) 1104-1112

[7] Clément F, Leng J "Evaporation of Liquids and Solutions in Confined Geometry" Langmuir 20 (2004) 6538-6541

[8] Daubersies L, Salmon JB "Evaporation of solutions and colloidal dispersions in confined droplets" Physical Review E 84 (2011) 031406

[9] Choi YS, Seo KW, MH Sohn, Lee SJ "Advances in digital holographic micro-PTV for analyzing microscale flows" Optics and Lasers in Engineering 50 (2012) 39-45

[10] Choi YS, Lee SJ "High-accuracy three-dimensional position measurement of tens of micrometers size transparent microspheres using digital in-line holographic microscopy" Optics Letters 36 (2011) 4167-4169